JACS
JOURNAL OF THE AMERICAN CHEMICAL SOCIETY

Article

pubs.acs.org/JACS

Ring-Opening Metathesis Polymerization with the Second Generation Hoveyda–Grubbs Catalyst: An Efficient Approach toward High-Purity Functionalized Macrocyclic Oligo(cyclooctene)s

Anton Blencowe and Greg G. Qiao*

Polymer Science Group, Department of Chemical and Biomolecular Engineering, The University of Melbourne, Parkville, Melbourne, Victoria 3010, Australia

Supporting Information

ABSTRACT: Herein, we present a facile and general strategy to prepare functionalized macrocyclic oligo(cyclooctene)s (cOCOEs) in high purity and high yield by exploiting the ring-opening metathesis polymerization (ROMP) intramolecular backbiting process with the commercially available second generation Hoveyda–Grubbs (**HG2**) catalyst. In the first instance, ROMP of 5-acetyloxycyclooct-1-ene (ACOE) followed by efficient quenching and removal of the catalyst using an isocyanide derivative afforded macrocyclic oligo(5-acetyloxycyclooct-1-ene) (cOACOE) in high yield (95%), with a weight-average molecular weight (M_w) of 1.6 kDa and polydispersity index (PDI) of 1.6, as determined by gel permeation chromatography (GPC). The structure and purity of the macrocycles were confirmed by NMR spectroscopy and elemental analysis, which indicated the complete absence of end-groups. This was further supported by GPC-matrix assisted laser desorption ionization time-of-flight mass spectroscopy (GPC-MALDI ToF MS), which revealed the exclusive formation of macrocyclic derivatives composed of up to 45 repeat units. Complete removal of residual ruthenium from the macrocycles was confirmed by inductively coupled plasma atomic emission spectroscopy (ICP-AES). The same methodology was subsequently extended to the ROMP of 5-bromocyclooct-1-ene and 1,5-cyclooctadiene to prepare their macrocyclic derivatives, which were further derivatized to produce a library of functionalized macrocyclic oligo(cyclooctene)s. A comparative study using the second and third generation Grubbs catalysts in place of the **HG2** catalyst for the polymerization of ACOE provided macrocycles contaminated with linear species, thus indicating that the bidendate benzylidene ligand of the Hoveyda–Grubbs catalyst plays an important role in the observed product distributions.

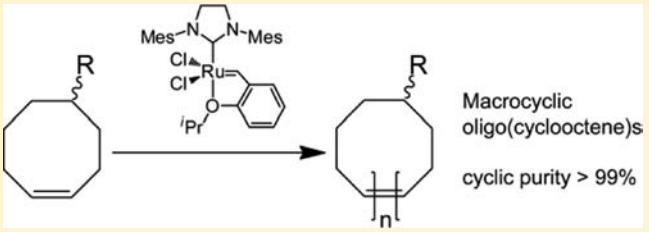

INTRODUCTION

As compared to their linear counterparts, cyclic polymers exhibit a number of unique physical properties that result from the topological restrictions imposed by a lack of chain ends.[1,2] For example, cyclic polymers display improved thermal, chemical, and biological stability,[3−5] lower intrinsic and melt viscosities,[3,6] favorable pharmacokinetics,[7] and remarkable self-assembling properties,[3,8] which makes them potential targets for a number of applications including drug delivery,[9] rheological modifiers, plasticizers, lubricants,[10] and as building blocks in polymer, supramolecular, and materials chemistry.[11,12] However, technical applications of cyclic polymers still remain limited due to the lack of inexpensive and commercially viable large-scale production methods. Of all of the reported methods for synthesizing cyclic polymers, ring-expansion polymerization is emerging as a promising candidate for the large-scale production of high-purity cyclic polymers.[1,2] Notable examples include the zwitterionic polymerization of cyclic esters and *N*-carboxyanhydrides using *N*-heterocyclic carbenes as catalysts,[13] and the ring-expansion metathesis polymerization (REMP) of strained cycloolefins using specially designed cyclic ruthenium catalysts.[11,14−17]

Although significant effort has been devoted to developing new approaches for the production of high molecular weight cyclic polymers and investigation of their structure-related properties, there is still substantial interest in developing versatile strategies for the preparation of high-purity macrocycles. Macrocycles have been employed in various fields as nonvolatile, thermally stable lubricants, hydraulic fluids and additives,[10] cosmetics,[18] sensors,[19] catalysts,[20] coordination complexes,[21] macrocyclic monomers for entropically driven ring-opening polymerization (ED-ROP),[22−24] and as building blocks for complex macromolecular architectures,[25] molecular recognition, and self-assembly.[22,26] Macrocyclic oligomers have long been observed as undesired side products in various polymerization systems, notably step-growth[22] and ring-opening polymerizations (ROP).[27,28] For ROP, intramolecular backbiting of linear polymer chains is responsible for the generation of low molecular weight cyclic and linear fragments and is in equilibrium with the formation of high molecular weight linear polymer chains. This ring–chain equilibrium is very sensitive to concentration, with high monomer concen-

Received: December 19, 2012
Published: March 26, 2013

dx.doi.org/10.1021/ja312418z | *J. Am. Chem. Soc.* 2013, 135, 5717−5725

trations favoring polymer formation and high dilution favoring macrocyclic oligomers. Perhaps one of the most widely studied ring−chain equilibriua is in ring-opening metathesis polymerization (ROMP),[27] whereby release of ring strain of cycloolefins provides an enthalpic driving force for irreversible ring-opening, although the formation of macrocycles through either cyclooligomerization or depolymerization remains prominent. Over 40 years of study has shown that the ring−chain equilibrium in ROMP is dependent upon a number of factors including the ring strain of the cycloolefin, the nature of the catalyst, the reaction conditions (i.e., temperature, solvent), and, most importantly, the monomer (i.e., cycloolefin) concentration. With refinement of the Jacobson−Stockmayer (JS) theory of ring−chain equilibria,[29,30] Suter and Höcker showed that it was possible to predict the equilibrium concentrations (JS-rotational isomeric state (RIS)) and proposed the concept of a critical monomer concentration ($[M]_c$) defined as the total amount of monomer per unit volume that gives rise to macrocycles at equilibrium.[31] Thus, when the initial monomer concentration is $<[M]_c$, only macrocycles and linear oligomers are formed, and when the concentration is $>[M]_c$, the equilibrium concentration of cyclics remains constant and linear polymer chains are formed. However, the JS-RIS model neglects ring-strain and as a result over predicts $[M]_c$. Therefore, Kornfield and co-workers further modified the model to take into account the ring-strain present in small ring cyclics, which allows more accurate prediction of the distribution of cyclics and linear products.[32] As such, a revised critical monomer concentration ($[M]_{c,\infty}$) was proposed and defined as the total monomer lost to cyclic products. In theory, if ROMP is conducted at a monomer concentration below $[M]_{c,\infty}$, low molecular weight oligomers will be formed, although the exact composition in terms of cyclic and linear oligomers may depend upon other factors. Although many studies have investigated the equilibrium between the formation of macrocyclics and high molecular weight linear polymer in ROMP,[27] to date, optimization of the intramolecular backbiting process has not been exploited as a general strategy to prepare high-purity macrocyclic cyclooctenes. Therefore, in this study, we assessed the feasibility of preparing high-purity macrocycles from readily available cyclooctene monomers and commercially available catalysts, with the aim of developing a simple and versatile method to prepare a library of macrocycles.

Previously, Grubbs and co-workers have demonstrated that REMP of strained cycloolefins (e.g., cyclooctene (COE), cyclododecatriene) using specially designed cyclic ruthenium catalysts provides access to high-purity cyclic polymers.[14−17] Interestingly, the REMP of COE in the first instance yielded cyclic poly(cyclooctene)s with molecular weights that were dependent upon the initial monomer to catalyst ([M]/[cat.]) ratio.[15] Given that in the absence of end-groups the molecular weight of the cyclic polymer should approach a thermodynamically stable state regardless of the [M]/[cat.] ratio, it was shown that catalyst degradation/deactivation prevents the equilibrium molecular weight from being achieved, even at high catalyst loadings ([M]/[cat.] = 33).[15] Although this approach provides access to high-purity cyclic polymers, the cyclic catalysts are not commercially available and require multistep synthesis.[16,33] Recently, Song et al. have demonstrated that macrocycles can be formed via alternating ROMP of cyclohexene and cyclobutene derivatives.[34] In their initial studies with the third generation Grubbs (**G3**) catalyst, they observed the formation of linear polymer contaminated with macrocyclic impurities generated through backbiting.[35] Subsequently, they employed the second generation Hoveyda−Grubbs (**HG2**) catalyst to increase the formation of macrocycles, which was hypothesized to result from the chelated structure of the catalyst stabilizing the transition state for backbiting at the styrenic terminus of the growing polymer chain.[34] Indeed, this approach does provide access to high-purity cyclics, although relatively high catalyst loadings and long reaction times are required, and the isolated yields were low, possibly as a consequence of difficulties in removing the catalyst from the macrocycles.[34] The application of commercially available catalysts is particularly appealing, especially if the isolated yields of macrocycles can be maximized without compromising their purity.

In this study, we investigate the ROMP of cyclooctene derivatives using the commercially available **HG2** catalyst and demonstrate a facile and general strategy to prepare functionalized macrocyclic oligo(cyclooctene)s (cOCOEs) in excellent yields and cyclic purity through optimization of the intramolecular backbiting process and efficient catalyst removal. In combination with a simple fractionation process, this synthetic strategy provides access to functionalized macrocycles with narrow molecular weight distributions in high isolated yields and free of residual ruthenium. Furthermore, we demonstrate efficient click functionalization of the macrocycles as a versatile approach toward the generation of libraries of functionalized macrocyclic building blocks. It is envisioned that the strategies introduced in this study will provide rapid access to functionalized macrocycles with applications in catalysis, coordination, and recognition systems, and as building blocks for more complex macromolecular architectures (e.g., multifunctional initiators for star polymers with cyclic cores) and self-assemblies. In addition, a detailed comparative study between the **HG2**, second generation Grubbs (**G2**), and **G3** catalysts was conducted to determine the effect of the catalyst structure on the purity of the macrocyclic product.

RESULTS AND DISCUSSION

Macrocyclic Oligo(5-acetyloxycyclooct-1-ene). As discussed previously, formation of macrocycles during the ROMP of cycloolefins generally results from intramolecular backbiting of growing polymer chains and leads to the establishment of a ring−chain equilibrium that is sensitive to the monomer concentration. Where well-defined linear polymer is desired, this process is disfavored as it leads to the contamination of the linear polymer and the formation of broad polydispersity products. However, if ROMP is conduced at concentrations below the $[M]_{c,\infty}$, then theoretically only a distribution of oligomers should be formed, although other factors may influence the topology of these oligomers (i.e., linear vs cyclic).[32] To establish a viable approach to prepare macrocycles, we investigated the polymerization of cyclooctene derivatives at concentrations that should favor intramolecular backbiting over chain growth. In the first instance, the ROMP of 5-acetyloxycyclooct-1-ene (ACOE) **1** to afford macrocycles was investigated using the **HG2** catalyst (Scheme 1), and the optimized conditions were subsequently extended to other cyclooctene derivatives.

Initially, ROMP of **1** was conducted at a monomer concentration of 0.2 M using the **HG2** catalyst ([**1**]:[**HG2**] = 120:1) as the $[M]_{c,\infty}$ for cyclooctene has been calculated to be 0.21 M.[32] However, at this concentration of **1**, the reaction resulted in a bimodal distribution of high and low molecular

dx.doi.org/10.1021/ja312418z | J. Am. Chem. Soc. 2013, 135, 5717−5725

Scheme 1. ROMP of ACOE 1 Using the HG2 Catalyst To Afford Macrocyclic OACOE M1[a]

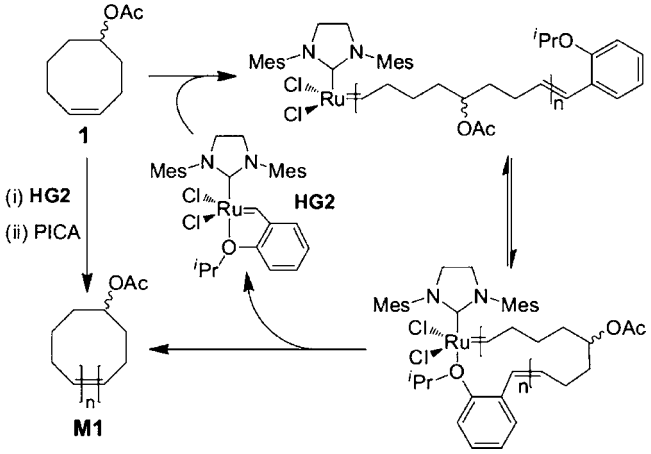

[a]Reagents and conditions: (i) [**1**] = 0.1 M in dichloromethane; [**1**]/[**HG2**] = 120, 60 min, 20 °C. (ii) PICA = potassium 2-isocyanoacetate; ACOE = 5-acetyloxycyclooct-1-ene **1**, **HG2** = second generation Hoveyda–Grubbs catalyst (Mes = 2,4,6-trimethylphenyl), OACOE = oligo(5-acetyloxycyclooct-1-ene).

weight products as determined from gel permeation chromatography (GPC) (Figure 1a, (i) and Supporting Information Figure S1) (low and high retention times, respectively), implying that the acetyloxy substituent of the monomer influences the ring strain and therefore $[M]_{c,\infty}$. When the reaction was repeated at a [**1**] of 0.1 M, the majority of the monomer was consumed in 60 min (>95% conversion by GCMS), leading to the formation of a low molecular weight product with a weight-average molecular weight (M_w) and polydispersity (PDI) of 1.6 kDa and 1.6, respectively (Figure 1a, (ii)). Attempts to quench the catalyst with the commonly employed ethyl vinyl ether (EVE) made separation of the catalyst from the oligomeric products exceedingly difficult as a result of their similar solubility characteristics. Furthermore, even when a large excess of EVE was employed, some of the catalyst remained active and resulted in the formation of high molecular weight polymer upon concentration of the crude reaction mixture (Supporting Information Figure S2). Therefore, the reaction was quenched by the addition of potassium 2-isocyanoacetate (PICA), which reacts with the catalyst to afford a water-soluble metathesis-inactive derivative[36] that could be readily separated from the oligomeric product by passing the quenched solution through a short plug of silica/basic alumina. As such, the product was isolated from the polymerization solution as a viscous transparent oil in high yield (95%) and displayed a GPC chromatogram identical to that of the reaction mixture before the reaction was quenched with PICA (Figure 1a, (ii)).

To assess the cyclic purity, the isolated product was subjected to ^{1}H NMR spectroscopic analysis and elemental analysis. ^{1}H NMR spectroscopic analysis of the polymer revealed resonances characteristic of oligo(5-acetyloxycyclooct-1-ene) (OACOE) at δ_H 4.83 and 5.34 ppm, corresponding to the methine protons adjacent to the acetate group and the alkene protons, respectively (Figure 1b). Surprisingly, no resonances were observed at low field (δ_H > 6.5 ppm), where aromatic proton resonances originating from end-groups derived from the bidentate isopropyloxybenzylidene ligand of the catalyst would be expected, thus indicating that the product consists

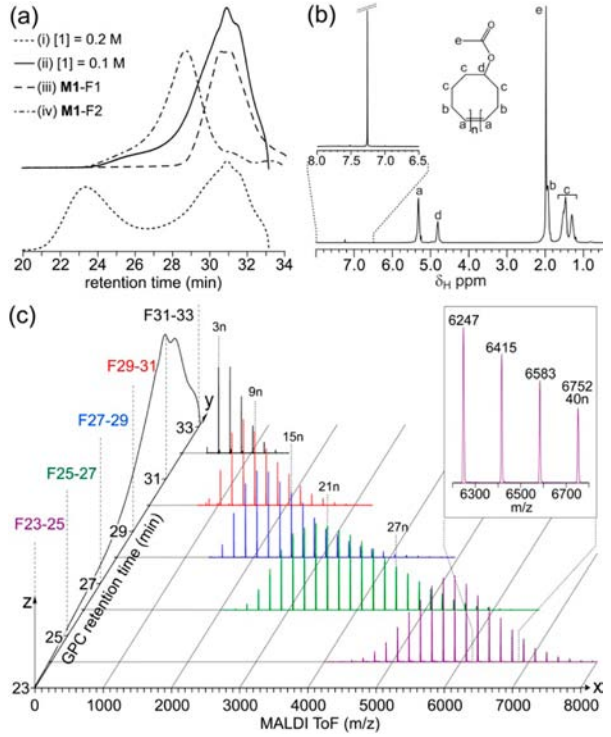

Figure 1. (a) GPC differential refractive index (DRI) chromatograms showing product distribution after ROMP of **1** at a monomer concentration of 0.2 and 0.1 M after 60 min of reaction, and macrocyclic OACOE **M1** after fraction into low (F1) and high (F2) molecular weight components. (b) ^{1}H NMR spectrum ($CDCl_3$) of **M1** isolated after 60 min of reaction and quenched with PICA, with expansion of the δ_H 6.5–8.0 ppm region. (c) GPC-MALDI ToF MS compilation showing mass spectra (*x*-axis) of the different time fractions collected from the GPC, as indicated in the GPC DRI chromatogram (*y*-axis). The *z*-axis refers to normalized intensity. Inset: Expansion of high mass region of fraction F23–25 mass spectrum showing the macrocyclic series (e.g., $[40n+Na]^+$ found, 6752.1 Da; calcd, 6752.2 Da). Mass spectra were recorded in linear/positive mode using *trans*-2-[3-(4-*tert*-butylphenyl)-2-methyl-2-propenylidene]-malononitrile (DCTB) as the matrix and sodium trifluoroacetate (NaTFA) as the cationization agent.

entirely of macrocyclic OACOE (**M1**). Elemental analysis provided further evidence for the high purity of the macrocycles with C and H values of 71.49% and 9.51%, respectively, which are very close to the calculated values for the pure macrocyclic (C, 71.39%; H, 9.59%). In comparison, the linear polymer with a comparable molecular weight would have C and H values of 73.34% and 9.41%, respectively, due to the influence of the end-groups. From these results, it can be concluded that under the conditions employed, backbiting to generate high-purity **M1** in high yield is the dominant process during ROMP with the **HG2** catalyst. To determine if residual ruthenium remained associated with macrocycle **M1**, it was extracted with 2 M nitric acid, and the aqueous extracts were subjected to inductively coupled plasma atomic emission spectroscopy (ICP-AES), which revealed the same background level of ruthenium as a control without **M1**.[37]

To determine the distribution and degree of polymerization (DP) of macrocycles, **M1** was subjected to matrix assisted laser desorption ionization time-of-flight mass spectrometry (MALDI ToF MS). Given the broad polydispersity of **M1**, initial attempts to obtain mass spectra representative of the

dx.doi.org/10.1021/ja312418z | J. Am. Chem. Soc. 2013, 135, 5717–5725

complete distribution of macrocyclics were hindered by mass discrimination against higher molecular weight components. Therefore, GPC coupled with MS (GPC-MALDI ToF MS) was conducted (Figure 1c) by collecting various time fractions (F23−25, F25−27, F27−29, F29−31, and F31−33 min) from the GPC and then analyzing them via MS. Because each time fraction only contains a narrow distribution of molecular weights, the mass discrimination effect observed for broad polydispersity polymers is minimized, therefore allowing for reliable analysis of the low intensity, higher molecular weight components of the sample. The mass spectra of each time fraction revealed a single series of peaks corresponding to **M1** (Figure 1c); even at higher molecular weights (F23−25 min), where the formation of linear polymer that had not undergone backbiting might be expected, there were no peaks corresponding to linear derivatives. The GPC-MALDI ToF MS results reveal that, although macrocycles with 3−15 repeat units are dominant, larger macrocycles with up to 45 repeat units (360 backbone atoms) are still formed. Although mass spectrometry coupled with chromatographic techniques have been used to investigate the DP of macrocyclics formed during ROMP of cyclooctene derivatives with various catalyst systems, only low DP values varying from 2−12 have been reported.[27,30] The much larger macrocyclics detected in the current study most likely result from the improved sensitivity of the GPC-MALDI ToF MS technique for detecting low intensity high molecular weight species, which has not previously been employed for such investigations. Another possibility is that the ability of the isopropyloxyaryl terminus of the growing polymer chain to chelate to the catalyst center favors backbiting at the end of the polymer chain rather than along the polymer backbone, thus leading to the formation of larger macrocyclics (vide infra).

To remove the quenched catalyst from the crude **M1** reaction mixture, the solution is passed through a short plug of silica/basic alumina. During this purification stage, **M1** could easily be separated into two fractions (a low and high mass) via elution with different solvents. Whereas elution with dichloromethane/pentane mixtures yielded a low molecular weight fraction (Figure 1a, (iii) **M1**-F1), elution with tetrahydrofuran (THF) provided a high molecular weight fraction (Figure 1a, (iv) **M1**-F2). MALDI ToF MS of **M1**-F1 and -F2 revealed single series of peaks, separated by the mass of the ACOE repeat unit (168.11 m/z) and with masses corresponding to macrocycles, and further confirmed the absence of linear contaminants (Figure 2). Because MALDI ToF MS can result in preferential ionization of species as a result of different end-groups (or no end-groups), it is conceivable that any linear species present in the polymer may not be observed in the MALDI ToF mass spectrum. Therefore, ESI MS was conducted to complement the MALDI ToF MS results, and revealed only peaks corresponding to macrocycles or their fragmented derivatives (Supporting Information Figures S3,4). The M_w of **M1**-F1 and -F2 as determined via mass spectrometry was 860 (PDI = 1.08) and 2200 Da (PDI = 1.11), respectively, which corresponds to an average DP of 5 and 13 per macrocycle, respectively. In comparison, GPC analysis of **M1**-F1 and -F2 (Figure 1a) using a conventional column calibration provided M_w values of 700 and 1600 Da. In general, cyclic polymers have higher retention in size exclusion chromatography than linear derivatives with the same molecular weight as a result of their smaller hydrodynamic volumes; however, it was not possible to directly compare linear and cyclic derivatives in this case as a result of the difficulty of obtaining pure linear OACOE of the required molecular weight. These results demonstrate that the polymerization of **1** with the **HG2** catalyst, combined with a simple quenching and fraction process, provides facile access to high-purity, narrow polydispersity macrocycles in high yield and free of residual ruthenium.

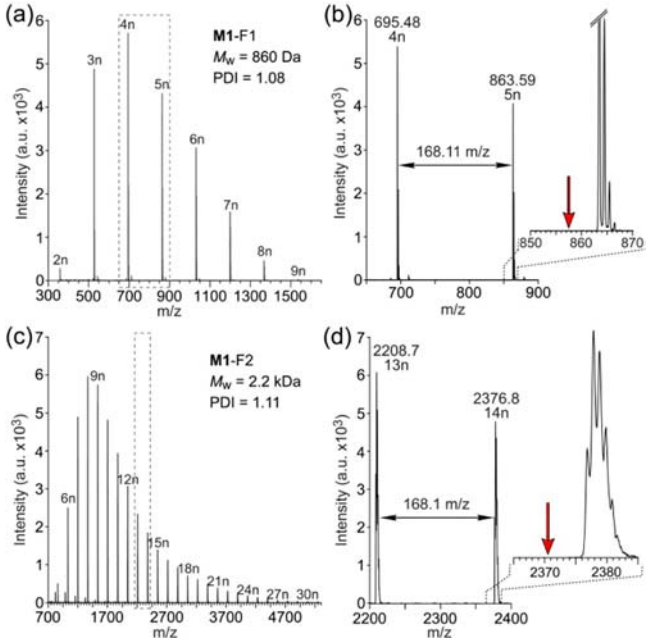

Figure 2. MALDI ToF mass spectra of **M1** (a,b) F1 and (c,d) F2 recorded in linear/positive mode using DCTB as the matrix and NaTFA as the cationization agent. The dashed boxes (a,c) refer to expanded regions (b,d). Vertical arrows (b,d) mark m/z values where linear polymer would be expected. All mass values correspond to Na^+ salts.

Functionalized Macrocyclic Libraries. To demonstrate that the methodology was applicable to other cyclooctene derivatives, 5-bromocyclooct-1-ene **2** and 1,5-cyclooctadiene **3** were polymerized to afford macrocyclic oligo(5-bromocyclooct-1-ene) **M2** and oligo(1,5-cyclooctadiene) **M3**, respectively (Scheme 2), in high yield and purity as evidenced by ^{1}H NMR spectroscopy, elemental analysis, and mass spectrometry. ^{1}H NMR spectroscopic analysis of **M2** and **M3** revealed characteristic resonances and a lack of resonances between δ_H 6.5−8.0 ppm confirming the absence of aryl end-groups (Figure 3a and b, respectively). Elemental analysis provided further evidence of the high purity of **M2** and **M3** with C and H values of 50.86% and 7.04%, and 89.09% and 11.11%, respectively (calcd **M2** C, 50.81%; H, 6.93%; **M3** C, 88.82%; H, 11.18%). As for **M1**, ICP-AES of **M2** and **M3** extracts also indicated that the macrocycles were free of residual ruthenium.[37] Attempts to analyze **M2** via mass spectrometry resulted in complex spectra as a result of significant fragmentation during the ionization process, although the ESI mass spectrum did reveal a series of peaks corresponding to macrocyclics and provided a M_w of 600 Da (PDI = 1.05) (Supporting Information Figure S5). Importantly, no peaks corresponding to linear derivatives were detected. MALDI ToF and ESI mass spectrometry of **M3** (Supporting Information Figure S6) both revealed series of peaks separated by 54.05 m/z units, which corresponds to one-half of a cyclooctadiene repeat unit (i.e., butene repeat unit) and results from backbiting at both double bonds of the cyclooctadiene repeat units during polymerization. As such, mass spectra of

dx.doi.org/10.1021/ja312418z | J. Am. Chem. Soc. 2013, 135, 5717−5725

Scheme 2. Synthesis of Macrocyclic Oligo(cyclooctene)s and Their Functionalized Derivatives via Copper-Mediated [2 + 3] Cycloaddition, Thiol−Ene Click, and Hydrolysis[a]

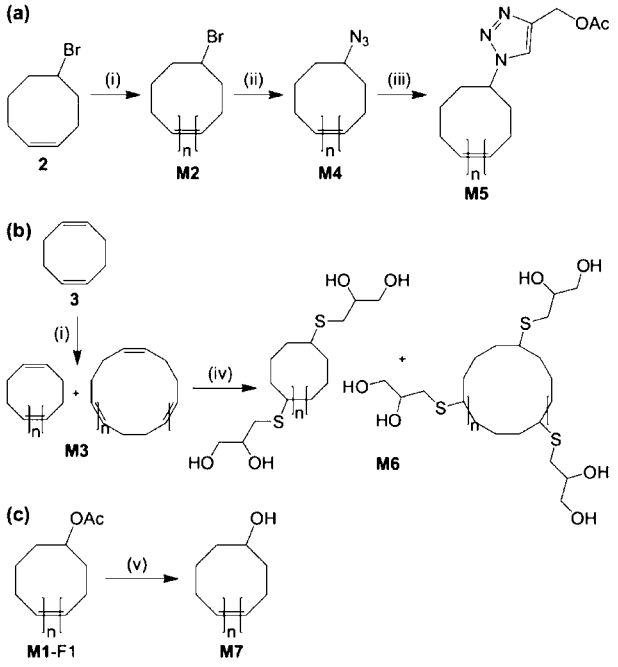

[a]Reagents and conditions: (i) **HG2**. (ii) NaN_3. (iii) $CuSO_4$, sodium ascorbate, prop-2-ynyl acetate. (iv) 2,2-Dimethoxy-2-phenylacetophenone, 1-thioglycerol, $h\nu$ (λ = 254 nm). (v) K_2CO_3.

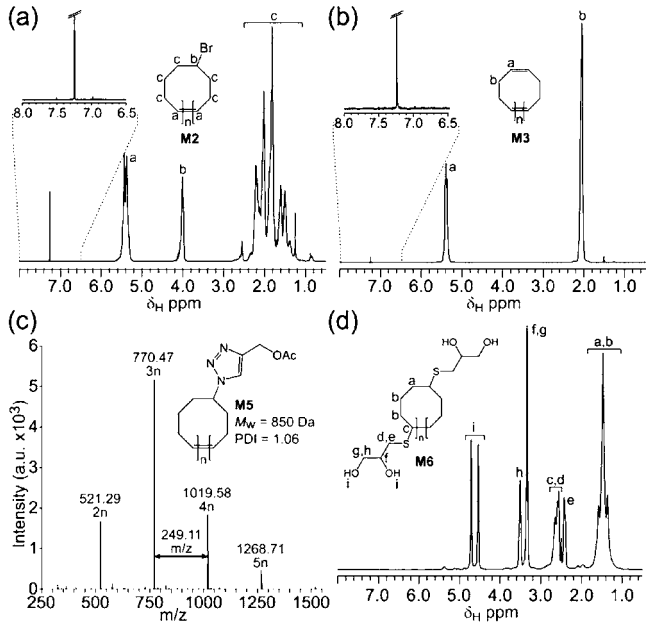

Figure 3. ^{1}H NMR spectra ($CDCl_3$) of (a) **M2** and (b) **M3**. (c) MALDI ToF mass spectra of click functionalized macrocycle **M5** recorded in linear/positive mode using DCTB as the matrix and NaTFA as the cationization agent. All mass values correspond to Na^+ salts. (d) ^{1}H NMR spectrum (d_6-DMSO) of thiol−ene functionalized macrocycle **M6**.

M3 contain series of cyclics with integers of the cyclooctadiene repeat unit (e.g., X*n*) and integers plus half (e.g., X.5*n*). Although linear oligo(1,5-cyclooctadiene) with end-groups derived from the catalyst has a mass nearly identical to that of the cyclic polymer, the lack of resonances corresponding to end-groups in the ^{1}H NMR spectrum confirms that the series observed in the mass spectra belong exclusively to cyclic polymer (Figure 3b). From MALDI ToF mass spectrometry, the M_w of **M3** was determined to be ca. 500−580 Da (PDI = 1.04−1.06) depending on the analysis conditions employed (Supporting Information Figure S6), which is consistent with the M_w (520 Da) determined by GPC (Supporting Information Figure S7).

The generalization of the described methodology to other cyclooctene derivatives provides a versatile platform from which to prepare families of macrocycles with varied functionalities. For example, conversion of **M2** to its azide derivative, macrocyclic oligo(5-azidocyclooct-1-ene) **M4**, facilitates further derivatization through [2 + 3] cycloaddition chemistries, or **M3** can be employed directly for thiol−ene click chemistries to generate highly functionalized derivatives. This was demonstrated via the conversion of **M2** to **M4** through reaction with NaN_3, followed by copper-mediated click with prop-2-ynyl acetate to afford the macrocyclic poly(cyclooctene triazole) derivative **M5** (Scheme 2a). Successful conversion of **M2** to the azido macrocyclic **M4** followed by click functionalization to afford the triazole macrocyclic **M5** was confirmed by ^{1}H NMR spectroscopic analysis (Supporting Information Figure S8), mass spectrometry (Figure 3c and Supporting Information Figures S9 and S10), and GPC (Supporting Information Figure S7). Whereas NMR spectroscopic analysis of **M5** revealed the complete disappearance of resonances corresponding to the methine protons adjacent to the azide groups of **M4** (Supporting Information Figure S8), MALDI ToF mass spectrometry of **M5** revealed a single series of peaks corresponding to the desired click functionalized macrocyclic (Figure 3c), which in combination provide a good indication that all of the functional transformations proceed efficiently with complete conversion. To prepare hydroxy functionalized macrocyclics, **M3** was reacted with thioglycerol in the presence of a radical photoinitiator (Scheme 2b). Analysis of the resulting macrocyclic polyol **M6** via ^{1}H NMR spectroscopic analysis revealed almost complete conversion (96%) of the alkenes of **M3** (Figure 3b) to thioethers (Figure 3d and Supporting Information Figure S11). The presence of unreacted alkene groups was also observed in the ESI mass spectrum (Supporting Information Figure S12), which provided a M_w of 980 Da (PDI = 1.07), similar to values determined by GPC (Supporting Information Figure S7). Alternatively, cyclic polyols could be generated from **M1** via hydrolysis of the acetyl groups to afford macrocyclic oligo(5-hydroxycyclooct-1-ene) **M7** (Scheme 2c). For example, hydrolysis of **M1**-F1 in the presence of potassium carbonate afforded **M7** quantitatively as determined by ^{1}H NMR spectroscopic analysis (Supporting Information Figure S13) and mass spectrometry (Supporting Information Figure S14). The facile synthesis of functionalized macrocyclic oligo(cyclooctene)s is anticipated to provide access to monomers and scaffolds for ED-ROP,[22−24] coordination complexes,[21] and complex macromolecular architectures with applications in catalysis,[20] polymer therapeutics,[38] and electronics.[39]

Influence of Catalyst on Macrocycle Formation. As suggested by Song et al., for ROMP with the **HG2** catalyst it appears likely that the ability of the isopropyloxyaryl terminus of the growing polymer chain to associate with the active ruthenium catalyst through an ether oxygen−metal type ligand interaction promotes backbiting by bringing the main chain

dx.doi.org/10.1021/ja312418z | J. Am. Chem. Soc. 2013, 135, 5717−5725

olefins in close contact to the metal alkylidene. This mechanism is supported by the studies of Vorfalt et al., which indicate that the rate-determining step for ruthenium metathesis catalysts with bidentate benzylidene-type ligands (e.g., **HG2** and Grela subtype catalysts) is olefin coordination to the metal center[40] rather than ligand dissociation as has been demonstrated with other ruthenium-based catalysts.[41] Therefore, the coordination of the isopropyloxyaryl terminus of the growing polymer chain to the metal center serves to bring the main chain olefins into close contact with the metal center, which does not rely on ligand dissociation prior to coordination of the olefin, but rather the olefin coordination promotes ligand dissociation. Previously, it has been shown that the rate-determining step in ROMP using the **G2** catalyst is ligand dissociation.[41] Because the liable tricyclohexylphosphine ligand is not incorporated into the growing polymer chain for ROMP with the **G2** catalyst, coordination of the free ligand to the metal center only leads to deactivation of the catalyst and does not bring the growing polymer chain into close proximity with the metal center. Therefore, the rate of intramolecular backbiting with the **G2** catalyst may be slower, increasing the probability of side reactions at the catalyst while it is still attached to the growing polymer chain. Thus, even at low monomer concentrations where macrocycle formation is favored, decomposition of the catalyst during its involvement in the catalytic cycle would lead to the formation of linear impurities.

To determine if the formation of pure macrocycles results solely from the monomer concentration employed or the effect of the catalyst structure and activation pathway, the ROMP of **1** at 0.1 M was repeated in a fashion identical to that described previously using the **G2** catalyst. The product was isolated as a very faint yellow viscous oil and subjected to ^{1}H NMR spectroscopic analysis and GPC-MALLS ToF MS. In comparison to the **HG2**-catalyzed reaction, the product isolated from the **G2**-catalyzed reaction displayed multiple resonances in the aromatic region of the NMR spectrum (Supporting Information Figure S15). Of particular note were doublet and double triplet resonances (ca. δ_H 6.35 and 6.15 ppm, respectively) characteristic of styrenic end-groups derived from the catalysts benzylidene ligand, thus indicating the presence of linear OACOE. GPC-MALLS ToF MS of the product was conducted in a fashion identical to that previously described (Supporting Information Figure S16). Whereas the GPC DRI chromatograms for the products isolated using both **HG2** and **G2** catalysts displayed similar profiles (Supporting Information Figure S17), MS analysis revealed significant differences. Although macrocycles dominate the product distribution at low masses (<2000 m/z), increasingly more series of peaks are observed toward higher masses. Conceivably, these series could result from fragmentation of the macrocycles during the mass spectroscopy ionization process; however, no such series are observed in the product isolated from the **HG2**-catalyzed reaction. Therefore, it is likely that these additional series result from linear OACOE with different end-groups, although it is not immediately apparent what structure these end-groups assume given that EVE was not used to quench the reaction. Galan et al. have demonstrated that isocyanides, like PICA, react with the **G2** catalyst to afford metathesis inactive derivatives, whereby two molecules of the isocyanide coordinate to the metal center and the benzylidene formally inserts into one of the mesityl groups of the *N*-heterocyclic carbene (NHC) ligand.[36] In the case of polymerization of **1**, any growing polymer chain present during quenching with PICA would be attached to a metal center via an alkylidene, which might be expected to insert into the mesityl group of the NHC ligand, deactivating the catalyst and preventing backbiting of the attached polymer to form macrocycles. Other possible sources of linear contamination may result from reaction of the polymer conjugated catalyst with methanol, which was used to dissolve the PICA prior to quenching. Previously, it has been demonstrated that Grubbs catalysts can react with primary alcohols, resulting in hydrogenation of the benzylidene group and the formation of ruthenium carbonyl species.[42] Such a reaction during polymerization would lead to release of the growing polymer chain from the catalyst and the formation of an alkyl end-group.

The presence of linear OACOE in the product isolated from the **G2**-catalyzed reaction implies that when the reaction is quenched some of the catalyst is involved in the polymerization cycle, whereas the lack of linear contamination in the **HG2**-catalyzed reaction product suggests that the catalyst resides predominantly in a dormant state during quenching. To study this possibility further, the reactions were repeated, and after 60 min a sample was directly analyzed via GPC without quenching. GPC coupled with UV−vis (λ = 370 nm) and DRI detection was employed to study the distribution of the catalyst relative to the OACOE product (Figure S17). For the **HG2**-catalyzed reaction, a single peak is observed in the UV−vis chromatogram corresponding to the free catalyst. In comparison, the UV−vis chromatogram of the **G2**-catalyzed reaction revealed two peaks, with one corresponding to free catalyst and the other overlapping with the peak for the polymer in the DRI chromatogram, which provides good evidence for the catalysts' attachment to growing polymer chains and involvement in the polymerization cycle. This observation supports the formation of linear OACOE during the polymerization of **1** with the **G2** catalyst, as quenching of these growing polymer chains with PICA would ultimately result in contamination of the macrocyclic OACOE with linear chains. The absence of linear OACOE for the **HG2**-catalyzed reaction suggests that the catalyst resides predominantly in a dormant state once the majority of the monomer has been consumed (ca. 60 min) and raises the possibility that an equilibrium state has been achieved.

To investigate the formation of linear contaminants and involvement of the catalyst at various stages of the polymerization, the polymerization of **1** at 0.1 M was studied via ^{1}H NMR spectroscopy using the **HG2** and **G2** catalysts, as well as the **G3** catalyst (Figure 4a−c, respectively). To assess the extent of the catalysts involvement in the formation of linear polymer chains, the benzylidene and styrenic proton regions of the spectra were monitored over time. Simultaneously, the conversion of **1** was also determined (Figure 4d) by monitoring the reduction in the monomers olefinic proton resonance. The ring-opening of **1** should initially result in the formation of a linear species with a styrenic end-group derived from the catalysts benzylidene ligand and an alkylidene end-group attached to the catalyst, and should be accompanied by the appearance of resonances in the ^{1}H NMR spectra corresponding to the styrenic end-group between δ_H 6.0 and 6.5 ppm and the disappearance of the benzylidene proton resonance of the original catalyst. For the **HG2** catalyst, no change in the benzylidene proton resonance at δ_H 16.5 ppm was observed over the first 60 min of reaction (95% monomer conversion), nor were any resonances observed corresponding to styrenic end-groups (Figure 4a), which confirms that the monomer is

dx.doi.org/10.1021/ja312418z | J. Am. Chem. Soc. 2013, 135, 5717−5725

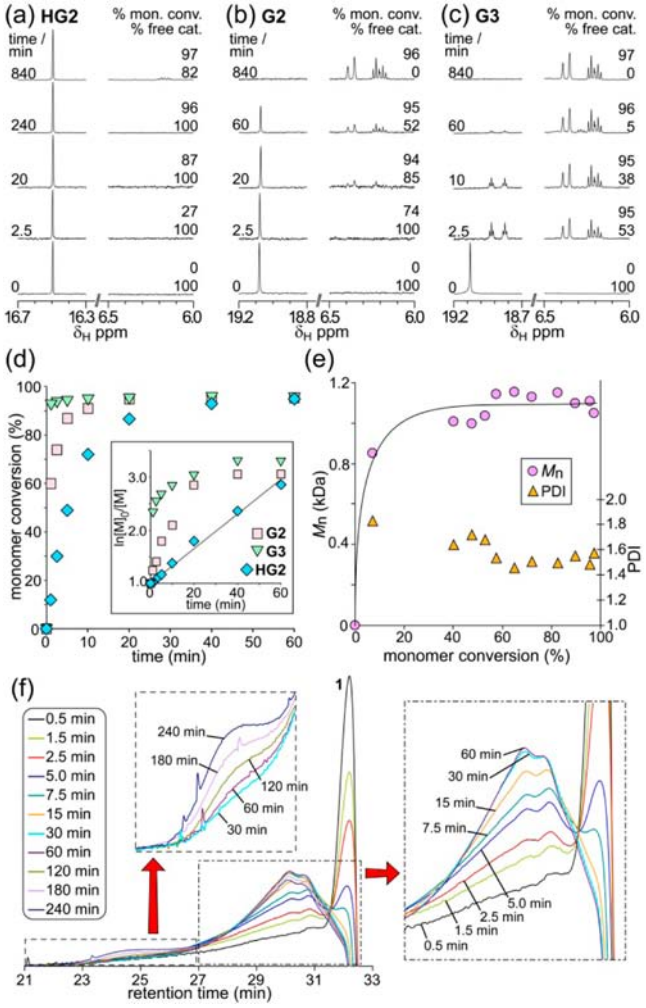

Figure 4. ^{1}H NMR spectra showing styrenic and benzylidene regions at various times during polymerization of **1** (0.1 M in CD_2Cl_2) using the (a) **HG2**, (b) **G2**, and (c) **G3** catalysts. (d) Monomer (**1**) conversion over a period of 60 min for polymerization of **1** (0.1 M in CD_2Cl_2) using the **HG2**, **G2**, and **G3** catalysts, as determined from ^{1}H NMR spectroscopic analysis; inset shows semilogarithmic kinetic plots. (e) Number-average molecular weight and polydispersity index (PDI) as a function of monomer conversion and (f) GPC DRI chromatograms recorded at different times for polymerization of **1** using the **HG2** catalyst.

converted solely to macrocycles with the catalyst only transiently entering the catalytic cycle before being regenerated. After 4 h of reaction, the monomer conversion increased slightly to 96%, and there were still no traces of linear polymer formation. However, at longer reaction times (14 h), the appearance of styrenic proton resonances at δ_H 6.2 ppm in the ^{1}H NMR spectrum indicates the formation of linear species. From comparison of the benzylidene proton resonances of the free catalyst and the styrenic proton resonances, it was determined that ca. 82% of the original catalyst remained after 14 h.

When the reaction was repeated using the **G2** catalyst, the rate of reaction increased significantly with 94% of the monomer being consumed in 20 min (Figure 4d). ^{1}H NMR spectra of the reaction revealed the appearance of styrenic proton resonances at δ_H 6.2 and 6.4 ppm at ca. 20 min, which intensified over time and implied that after 60 min of reaction ca. 50% of the catalyst was involved in the formation of linear polymers chains.

These observations are consistent with both the mass spectroscopy and the GPC-UV results and support the presence of linear contaminants in the macrocycles isolated from polymerization of **1** with the **G2** catalyst after 60 min of reaction. After 14 h, none of the original catalyst was detected, implying that it was either conjugated to linear polymer chains or had undergone degradation. Therefore, as might be expected under the conditions employed, the **G2** catalyst affords macrocycles as the dominant reaction products, even at relatively high monomer conversions (<94%), and could also be employed to prepare high-purity macrocycles if the reaction time is carefully controlled. In comparison, the formation of linear contaminants in the **HG2**-catalyzed reaction is negligible even at long reaction times and high monomer conversions, which is attributed to the ligand-mediated backbiting mechanism described previously. Therefore, at low monomer concentrations, the **HG2** catalyst behaves similarly to cyclic REMP catalysts[15] and allows the preparation of pure macrocycles in high yields. Further studies are currently underway to determine the effect that the catalyst structure has on the product distribution (i.e., linear vs cyclic) at higher monomer concentrations.

Previously, it has been reported that polymerization of cyclooctene derivatives at a monomer concentration of 0.1 M using the **G3** catalyst initially results in the formation of linear polymers that undergo cyclodepolymerization to afford macrocycles exclusively.[20] ^{1}H NMR spectra of the polymerization of **1** with the **G3** catalyst (Figure 4c) revealed the almost instantaneous formation of styrenic proton resonances at δ_H 6.2 and 6.4 ppm, and after 2.5 min 95% of the monomer had been consumed (Figure 4d) with ca. 50% of the catalyst involved in linear polymer formation. Although the monomer conversion did not significantly increase at longer reaction times, the amount of catalyst involved in linear polymer formation increased to 95% after 60 min (Figure 4c). In addition, the near complete disappearance of the carbene proton resonances at ca. δ_H 18.8 and 18.9 ppm after 60 min suggests degradation of the majority of active carbene species, which is not surprising given the lower stability of the **G3** catalyst relative to the **G2** and **HG2** catalysts.[43] These results suggest that even though cyclodepolymerization to afford macrocycles becomes dominant at high monomer conversions,[20] linear species remain present throughout the reaction and would ultimately lead to contamination of the macrocycles. The initial formation of large molecular polymers prior to cyclodepolymerization to afford macrocycles observed with **G3** is attributed to the catalysts very high initiation rate[43] and is in contrast to the behavior of the **G2** and **HG2** catalyst.

For the **HG2** catalyst, polymerization of **1** at low monomer conversions (<10%) initially leads to formation of macrocycles with a broad polydispersity (PDI = 1.8) and a M_n of ca. 800 Da (Figure 4e). At higher monomer conversions (>40%), the polydispersity decreases slightly, and the M_n remains constant at ca. 1.1 kDa. GPC DRI chromatograms recorded over time revealed several different growth regions depending on the reaction time and monomer conversion (Figure 4f). For example, at low monomer conversions (<20%; ca. 2 min), both high and low molecular weight macrocycles with retention times of 23−27 and 27−31 min are formed, whereas consumption of the remaining monomer contributes predominantly to the formation of low molecular weight species.

dx.doi.org/10.1021/ja312418z | J. Am. Chem. Soc. 2013, 135, 5717−5725

Interestingly, at high monomer conversions (>95%), an increase in the high molecular weight species is observed and is accompanied by a decrease in the low molecular weight species. These results imply that initially cyclopolymerization dominates to afford small to large macrocycles, and as the monomer is depleted, backbiting and catalyst release becomes more prominent relative to propagation, resulting in the generation of smaller macrocycles. Once the majority of the monomer is consumed, the smaller macrocycles re-enter the catalytic cycle, undergoing intermolecular chain transfer to afford larger macrocycles, in a fashion similar to that observed for certain cyclic REMP catalysts.[15] This latter observation suggests that the macrocycles are yet to reach the ring size having the lowest thermodynamic energy under the conditions employed, and raises the possibility that at longer reaction times the **HG2** catalyst could be employed to prepare higher molecular weight macrocycles.

CONCLUSIONS

In summary, we have demonstrated that ring-opening metathesis polymerization of cyclooctene derivatives using the second generation Hoveyda−Grubbs catalyst below the critical monomer concentration results exclusively in the formation of macrocycles with up to 45 repeat units. Quenching of the catalyst with potassium 2-isocyanoacetate allowed for efficient removal of the catalyst and rapid isolation of macrocyclics free of residual ruthenium and in very high yields. The methodology was shown to be generalizable to various cyclooctenes, to produce macrocycles suitable for derivatization via click chemistry approaches. As demonstrated through the quantitative copper-mediated azide−alkyne cycloaddition of an azide-functionalized macrocycle and the radical-mediated thiol−ene click of oligo(cyclooctadiene) to afford macrocyclic polyols, the ability to prepare functionalized macrocyclics in high purity and yield is anticipated to allow access to families of macrocycles suitable for catalysis, coordination and recognition systems, monomers for entropically driven ring-opening polymerization, and building blocks for more complex macromolecular architectures and self-assemblies. A detailed comparison between different Grubbs catalysts revealed that unlike the second generation Hoveyda−Grubbs catalyst, the second and third generation Grubbs catalysts are more prone to residing in the catalytic cycle at high monomer conversions, leading to contamination of the isolated macrocycles with linear oligomers. The absence of linear oligomers in the second generation Hoveyda−Grubbs-catalyzed reaction implies that the catalyst only resides transiently in the catalytic cycle. This behavior is attributed to the bidendate benzylidene ligand of the catalyst, which upon entering the catalytic cycle is able to promote efficient backbiting via coordination of the isopropyloxyaryl terminus of the growing polymer chain with the metal center to release the macrocycle and regenerate the catalyst. Therefore, application of the second generation Hoveyda−Grubbs catalyst for the synthesis of high-purity macrocycles is favorable.

ASSOCIATED CONTENT

Supporting Information

Materials, instrumentation, and synthetic procedures, MALDI ToF and ESI mass spectra, GPC chromatograms, and NMR spectra. This material is available free of charge via the Internet at http://pubs.acs.org.

AUTHOR INFORMATION

Corresponding Author

gregghq@unimelb.edu.au

Notes

The authors declare no competing financial interest.

ACKNOWLEDGMENTS

This work was supported by the Australian Research Council (ARC) under the Discovery Project (DP0984915) scheme. The MALDI ToF MS used in these studies was supported under the ARC's Linkage Infrastructure, Equipment and Facilities funding (LE0882576) scheme. We are grateful to Dr. Tor Kit Goh (The University of Melbourne) for helpful discussion and Dr. Troy Attard (Bio21 Institute, The University of Melbourne) for technical assistance.

REFERENCES

(1) (a) Jia, Z.; Monteiro, M. J. *J. Polym. Sci., Part A: Polym. Chem.* **2012**, *50*, 2085−2097. (b) Laurent, B. A.; Grayson, S. M. *Chem. Soc. Rev.* **2009**, *38*, 2202−2213.

(2) Kricheldorf, H. R. *J. Polym. Sci., Part A: Polym. Chem.* **2010**, *48*, 251−284.

(3) Yamamoto, T.; Tezuka, Y. *Polym. Chem.* **2011**, *2*, 1930−1941.

(4) Chen, R.; Nossarev, G. G.; Hogen-Esch, T. E. *J. Polym. Sci., Part A: Polym. Chem.* **2004**, *42*, 5488−5503.

(5) De Rosa, M.; Gambacorta, A. *Prog. Lipid Res.* **1988**, *27*, 153−175.

(6) Clarson, S. J.; Semlyen, J. A. *Polymer* **1986**, *27*, 1633−1636.

(7) Nasongkla, N.; Chen, B.; Macaraeg, N.; Fox, M. E.; Fréchet, J. M. J.; Szoka, F. C. *J. Am. Chem. Soc.* **2009**, *131*, 3842−3843.

(8) Honda, S.; Yamamoto, T.; Tezuka, Y. *J. Am. Chem. Soc.* **2010**, *132*, 10251−10253.

(9) Fox, M. E.; Szoka, F. C.; Fréchet, J. M. J. *Acc. Chem. Res.* **2009**, *42*, 1141−1151.

(10) (a) Bahr, S. R.; Doyle, N.; Wang, J.; Winckler, S. J.; Takekoshi, T.; Wang, Y.-F. US 20070216067, 2007. (b) Hampton, J. F. U.S. patent 3465016, 1967.

(11) (d) Zhang, K.; Lackey, M. A.; Cui, J.; Tew, G. N. *J. Am. Chem. Soc.* **2011**, *133*, 4140−4148.

(12) Laurent, B. A.; Grayson, S. M. *J. Am. Chem. Soc.* **2011**, *133*, 13421−13429.

(13) (a) Jeong, W.; Hedrick, J. L.; Waymouth, R. M. *J. Am. Chem. Soc.* **2007**, *129*, 8414−8415. (b) Shin, E. J.; Brown, H. A.; Gonzalez, S.; Jeong, W.; Hedrick, J. L.; Waymouth, R. M. *Angew. Chem., Int. Ed.* **2011**, *50*, 6388−6391. (c) Jeong, W.; Shin, E. J.; Culkin, D. A.; Hedrick, J. L.; Waymouth, R. M. *J. Am. Chem. Soc.* **2009**, *131*, 4884−4891. (d) Lee, C.-U.; Smart, T. P.; Guo, L.; Epps, T. H.; Zhang, D. *Macromolecules* **2011**, *44*, 9574−9585. (e) Guo, L.; Zhang, D. *J. Am. Chem. Soc.* **2009**, *131*, 18072−18074.

(14) (a) Bielawski, C. W.; Benitez, D.; Grubbs, R. H. *Science* **2002**, *297*, 2041−2044.

(15) (b) Xia, Y.; Boydston, A. J.; Yao, Y.; Kornfield, J. A.; Gorodetskaya, I. A.; Spiess, H. W.; Grubbs, R. H. *J. Am. Chem. Soc.* **2009**, *131*, 2670−2677.

(16) (c) Boydston, A. J.; Xia, Y.; Kornfield, J. A.; Gorodetskaya, I. A.; Grubbs, R. H. *J. Am. Chem. Soc.* **2008**, *130*, 12775−12782.

(17) (e) Bielawski, C. W.; Benitez, D.; Grubbs, R. H. *J. Am. Chem. Soc.* **2003**, *125*, 8424−8425.

(18) Rountree, S. M.; Lagunas, M. C.; Hardacre, C.; Davey, P. N. *Appl. Catal., A* **2011**, *408*, 54−62.

(19) Xue, G.; Savage, P. B.; Bradshaw, J. S.; Zhang, X. X.; Izatt, R. M. *Adv. Supramol. Chem.* **2000**, *7*, 99−137.

(20) Zheng, X.; Jones, C. W.; Weck, M. *J. Am. Chem. Soc.* **2007**, *129*, 1105−1112.

(21) (a) Park, S.-H.; Lee, S.-Y.; Park, K.-M.; Lee, S.-S. *Acc. Chem. Res.* **2012**, *45*, 391−403. (b) Hancock, R. D.; Maumela, H.; de Sousa, A. S. *Coord. Chem. Rev.* **1996**, *148*, 315−347.

(22) Hodge, P. *React. Funct. Polym.* **2001**, *48*, 15−23.

(23) Xue, Z.; Mayer, M. F. *Soft Matter* **2009**, *5*, 4600−4611.
(24) Strandman, S.; Gautrot, J. E.; Zhu, X. X. *Polym. Chem.* **2011**, *2*, 791−799.
(25) Dria, R. D.; Goudy, B. A.; Moga, K. A.; Corbin, P. S. *Polym. Chem.* **2012**, *3*, 2070−2081.
(26) (a) Baillargeon, P.; Bernard, S.; Gauthier, D.; Skouta, R.; Dory, Y. L. *Chem.-Eur. J.* **2007**, *13*, 9223−9235. (b) Rambo, B. M.; Gong, H.-Y.; Oh, M.; Sessler, J. L. *Acc. Chem. Res.* **2012**, *45*, 1390−1401. (c) Gibson, S. E.; Lecci, C. *Angew. Chem., Int. Ed.* **2006**, *45*, 1364−1377.
(27) Monfette, S.; Fogg, D. E. *Chem. Rev.* **2009**, *109*, 3783−3816.
(28) (a) Lecomte, P.; Jérôme, C. *Adv. Polym. Sci.* **2012**, *245*, 173−218. (b) Kricheldorf, H. R. *Macromol. Rapid Commun.* **2009**, *30*, 1371−1381. (c) Ren, M. R.; Fu, Q.; Blencowe, A.; Qiao, G. G. *ACS Macro Lett.* **2012**, *1*, 681−686.
(29) Jacobson, H.; Stockmayer, W. H. *J. Chem. Phys.* **1950**, *18*, 1600−1606.
(30) Ivin, K. J.; Mol, J. C. *Olefin Metathesis and Metathesis Polymerization*; Academic Press: New York, 1997.
(31) Suter, U. W.; Höcker, H. *Makromol. Chem.* **1988**, *189*, 1603−1612.
(32) Chen, Z.-R.; Claverie, J. P.; Grubbs, R. H.; Kornfield, J. A. *Macromolecules* **1995**, *28*, 2147−2154.
(33) Fürstner, A.; Ackermann, L.; Gabor, B.; Goddard, R.; Lehmann, C. W.; Mynott, R.; Stelzer, F.; Thiel, O. R. *Chem.-Eur. J.* **2001**, *7*, 3236−3253.
(34) Song, A.; Parker, K. A.; Sampson, N. S. *Org. Lett.* **2010**, *12*, 3729−3731.
(35) Song, A.; Parker, K. A.; Sampson, N. S. *J. Am. Chem. Soc.* **2009**, *131*, 3444−3445.
(36) Galan, B. R.; Kalbarczyk, K. P.; Szczepankiewicz, S.; Keister, J. B.; Diver, S. T. *Org. Lett.* **2007**, *9*, 1203−1206.
(37) To validate the extraction method, a sample of **M1** was spiked with the **HG2** catalyst that had been reacted with PICA and subjected to the same extraction process, which resulted in >98% extraction of the ruthenium.
(38) (a) Wiltshire, J. T.; Qiao, G. G. *Aust. J. Chem.* **2007**, *60*, 699−705. (b) Qiu, L. Y.; Wang, R. J.; Zheng, C.; Jin, Y.; Jin, L. Q. *Nanomedicine* **2010**, *5*, 193−208. (c) Dai, X.-H.; Dong, C.-M.; Fa, H.-B.; Yan, D.; Wei, Y. *Biomacromolecules* **2006**, *7*, 3527−3533. (d) Liu, T.; Li, X.; Qian, Y.; Hu, X.; Liu, S. *Biomaterials* **2012**, *33*, 2521−2531.
(39) Kanibolotsky, A. L.; Perepichka, I. F.; Skabara, P. J. *Chem. Soc. Rev.* **2010**, *39*, 2695−2728.
(40) Vorfalt, T.; Wannowius, K.-J.; Plenio, H. *Angew. Chem., Int. Ed.* **2010**, *49*, 5533−5336.
(41) Sanford, M. S.; Ulman, M.; Grubbs, R. H. *J. Am. Chem. Soc.* **2001**, *123*, 749−750.
(42) (a) Dinger, M. B.; Mol, J. C. *Organometallics* **2003**, *22*, 1089−1095. (b) Dinger, M. B.; Mol, J. C. *Eur. J. Inorg. Chem.* **2003**, 2827−2833.
(43) Love, J. A.; Morgan, J. P.; Trnka, T. M.; Grubbs, R. H. *Angew. Chem., Int. Ed.* **2002**, *41*, 4035−4037.